

This is the accepted manuscript made available via CHORUS. The article has been published as:

Indirect determination of neutron capture cross sections on spherical and near-spherical nuclei using the surrogate method

B. L. Goldblum, M. Wiedeking, T. Reed, K. Alfonso, J. M. Allmond, L. A. Bernstein, D. L. Bleuel, F. S. Dietrich, R. Hatarik, P. T. Lake, I.-Y. Lee, S. R. Lesher, S. Paschalis, M. Petri, L. Phair, N. D. Scielzo, R. Vial, and J. Vujic

Phys. Rev. C **85**, 054616 — Published 17 May 2012

DOI: [10.1103/PhysRevC.85.054616](https://doi.org/10.1103/PhysRevC.85.054616)

Indirect determination of neutron capture cross sections on spherical and near-spherical nuclei using the surrogate method

B.L. Goldblum,^{1,2,3} M. Wiedeking,^{4,5} T. Reed,² K. Alfonso,¹ J.M. Allmond,^{6,7} L.A. Bernstein,⁴ D.L. Bleuel,⁴ F.S. Dietrich,⁴ R. Hatarik,⁴ P.T. Lake,³ I.-Y. Lee,³ S.R. Leshner,⁴ S. Paschalis,³ M. Petri,³ L. Phair,³ N.D. Scielzo,⁴ R. Vial,^{1,8} and J. Vujic¹

¹*Department of Nuclear Engineering, University of California, Berkeley, California 94720, USA*

²*Department of Nuclear Engineering, University of Tennessee, Knoxville, Tennessee 37996, USA*

³*Nuclear Science Division, Lawrence Berkeley National Laboratory, Berkeley, California 94720, USA*

⁴*Lawrence Livermore National Laboratory, Livermore, California 94551, USA*

⁵*iThemba LABS, P.O. Box 722, Somerset West 7129, South Africa*

⁶*Joint Institute for Heavy Ion Research, Oak Ridge National Laboratory, Oak Ridge, Tennessee 37831, USA*

⁷*Department of Physics, University of Richmond, Virginia 23173, USA*

⁸*Grenoble INP - Phelma, 38016 Grenoble Cedex 1, France*

(Dated: May 3, 2012)

The $^{92}\text{Mo}(n,\gamma)$ cross section was obtained using both the absolute surrogate approach and surrogate ratio method (SRM), relative to the $^{94}\text{Mo}(n,\gamma)$ cross section, in an equivalent neutron energy range of 80 to 890 keV. Excited ^{93}Mo and ^{95}Mo nuclei were populated using the $^{92}\text{Mo}(d,p)$ and $^{94}\text{Mo}(d,p)$ reactions, respectively. Both discrete and statistical tagging approaches were employed to identify the γ -decay channel and were examined in terms of their sensitivity to the initial angular momentum population distribution. The absolute surrogate $^{92}\text{Mo}(n,\gamma)$ cross sections disagree with evaluated neutron capture cross section data by as much as a factor of four, whereas the results obtained using the SRM trend more favorably with the evaluated result. Experimental results suggest that discrete and statistical tagging approaches may sample different contributions of the γ -cascade for near-spherical nuclei. This work represents the first use of the surrogate method in the determination of neutron capture cross sections on spherical and quasi-spherical nuclei in the mass-90 region and provides a possible pathway to extend the SRM to a broader mass range.

PACS numbers: 24.10.-i, 24.87.+y, 29.30.Kv

I. INTRODUCTION

The surrogate method appears to be a promising technique in that neutron-induced fission cross sections have been obtained using the surrogate ratio method (SRM) for both stable and radioactive nuclei from energies of several hundred keV up to 20 MeV with total uncertainties on the order of 10% or less [1–7]. This effort was recently expanded to include the determination of neutron capture cross sections. Two approaches have been applied to tag the γ -decay channel in the indirect determination of neutron capture cross sections using the surrogate method: discrete tagging [8–11] and statistical tagging [12, 13].

In a discrete tagging approach, a known transition in the compound nucleus is used to identify the γ -decay channel. This method yields low statistics, but the ability to unequivocally tag the compound nucleus removes any potential contributions resulting from target impurities. In contrast, using a statistical tagging approach, the γ -decay probability is obtained by determining the total number of γ rays in a given energy range detected as a function of excitation energy. This approach has the advantage that low-resolution, high-efficiency γ -ray detectors may be employed and thus significantly higher statistics may be achieved. However, a statistical tagging approach is sensitive to potential target contamination. Each approach can vary in terms of execution

(e.g., model-dependent vs. model-independent, reliance on empirical data, etc.) and in the normalization of the γ -decay probabilities (e.g., via photon detection efficiency, assumption of unit probability below the neutron separation energy, etc.).

The $^{92}\text{Mo}(d,p)$ and $^{94}\text{Mo}(d,p)$ reactions were performed at the 88-Inch Cyclotron at Lawrence Berkeley National Laboratory using an array of five Compton-suppressed high-purity Germanium (HPGe) detectors to detect the de-excitation γ rays. The surrogate $^{92}\text{Mo}(n,\gamma)$ cross section was obtained using the absolute surrogate technique and, separately, via the SRM relative to the $^{94}\text{Mo}(n,\gamma)$ cross section, representing the first use of the surrogate method in the determination of neutron capture cross sections on spherical or near-spherical nuclei. Both discrete and statistical γ -ray tagging approaches were employed, with normalization of the γ -decay probabilities performed using the measured absolute photon detection efficiency of the HPGe array.

The ^{92}Mo and ^{94}Mo target nuclei ($Z = 42$) are located at and near the $N = 50$ neutron shell closure and have quadrupole moments that are approximately zero (cf. $Q(2^+; ^{94}\text{Mo}) = -0.13(8) \text{ e b}$ or $+0.01(8) \text{ e b}$ [14]). In general, the surrogate technique is based on the Weisskopf-Ewing approximation [15], which requires that the energy of the compound nucleus is sufficiently high that essentially all channels into which it can decay are dominated by integrals over the level density (i.e.,

the fraction of decays proceeding to resolved states is small). This is a statistical regime where the level density is reasonably described by a continuous function and all final spin states are equally represented. In general, more deformed nuclei have a higher low-energy level density compared with spherical nuclei and the applicability of the surrogate method in the Weisskopf-Ewing limit may extend to lower excitation energies for deformed nuclei as a result. If the Weisskopf-Ewing approximation is not valid, the γ -decay probabilities extracted via the surrogate technique are particularly sensitive to the angular momentum population distribution in the compound nucleus and significant deviations could be expected between the directly measured and surrogate neutron capture cross section data [16].

II. METHODOLOGY

In the Weisskopf-Ewing limit, the expression for the excitation-energy dependent neutron-induced γ -decay cross section in terms of the surrogate reaction γ -decay probability is given by

$$\sigma_{(n,\gamma)}(E_n) = \sigma_n^{CN}(E_n) P_{\beta\gamma}(E_x), \quad (1)$$

where E_n is the incident neutron energy, E_x is the excitation energy in the compound nucleus and $\sigma_n^{CN}(E_n)$ is the neutron-induced compound nuclear formation cross section [17]. $P_{\beta\gamma}(E_x)$ is the γ -decay probability for the compound nucleus formed via the surrogate reaction, labeled β with $\beta = (d, p)$ here, and can be written as

$$P_{\beta\gamma}(E_x) = \frac{N_{\beta\gamma}(E_x)}{N_\beta(E_x)}, \quad (2)$$

where $N_{\beta\gamma}(E_x)$ is the number of γ -cascades in coincidence with the surrogate reaction ejectile and $N_\beta(E_x)$ is the number of surrogate reaction events, both a function of excitation energy, where

$$E_x = S_n + \frac{A}{A+1} E_n, \quad (3)$$

S_n is the neutron separation energy in the compound nucleus and A is the mass of the target nucleus in the neutron-induced reaction.

For the absolute surrogate measurement, the neutron-induced ^{93}Mo compound-nuclear formation cross section, $\sigma_n^{CN}(E_n)$, was calculated using an optical model formalism employing the Koning-Delaroche global optical potential [18]. The uncertainty in the compound formation cross section calculation is approximated as 10% over the entire equivalent neutron energy range examined.

An accurate measurement of the total number of surrogate reaction events is contingent upon the purity of the target. Reactions on target contaminants will increase the ostensible number of direct reaction events, resulting in a measured γ -decay probability that is lower than the

true probability. The total number of surrogate reaction events is given by

$$N_\beta(E_x) = \sigma_\beta(E_x) \rho \int_0^{\Delta t} I(t) \ell(t) dt, \quad (4)$$

where $\sigma_\beta(E_x)$ is the cross section for forming the compound nucleus via the surrogate reaction, ρ represents the areal target density, I is the beam intensity delivered to the target in particles per unit time, ℓ is the live time fraction of the data acquisition system and Δt is the elapsed time for data collection. The parameters ρ , I , ℓ and Δt can be determined directly from experimental data. However, calculations of $\sigma_\beta(E_x)$ at the excitation energies relevant for surrogate measurements are particularly difficult, due to the high level densities and lack of nuclear structure data in the region. Thus, $N_\beta(E_x)$ was measured directly as the total number of $^{92}\text{Mo}(d, p)$ events. The possible presence of target contamination is addressed in Sec. IV.

For each 100 keV excitation energy bin in the compound nucleus, γ -ray spectra covering an energy range of approximately 100 keV to 8 MeV were recorded. Each γ -ray spectrum was convolved with the measured absolute γ -ray detection efficiency, $\epsilon(E_\gamma)$. A detailed absolute γ -ray detection efficiency calibration was performed for the HPGe array, using a ^{152}Eu sealed source at low γ -ray energies and via the $^{12}\text{C}(d, p)^{13}\text{C}$ and $^{13}\text{C}(d, p)^{14}\text{C}$ reactions for higher γ -ray energies, as described in Ref. [19]. The number of γ -cascades in coincidence with the surrogate reaction ejectile was estimated using both a discrete and statistical γ -decay tagging approach. For the present discrete tagging approach, the area of the lowest-lying transition in the ^{93}Mo residual nucleus at 943.28 keV, $1/2^+ \rightarrow 5/2^+$, (and for the surrogate ratio measurement, in the ^{95}Mo residual nucleus at 204.12 keV, $3/2^+ \rightarrow 5/2^+$, as discussed below), was used to tag the γ -decay channel. This is formally expressed as follows

$$N_{\beta\gamma}^{disc}(E_x) = \int_{peak} \frac{N'_{\beta\gamma}(E_x, E_\gamma)}{\epsilon(E_\gamma)} dE_\gamma P_{disc}, \quad (5)$$

where $N'_{\beta\gamma}(E)$ represents the number of particle- γ coincident events measured and P_{disc} represents the probability that the γ -cascade resultant from the initial angular momentum population distribution passes through the particular discrete transition of interest.

Using the statistical tagging approach, the total number of γ -rays in the energy range between 6 – 7 MeV was used to tag the γ -decay channel, corrected for Compton contribution using a shelf-model. The 6 – 7 MeV γ -ray energy range was chosen as it is above the average γ -ray energy expected from de-excitation from a level at the positive equivalent neutron energies relevant for this measurement in both ^{93}Mo and ^{95}Mo compound nuclei, as calculated using the model of Døssing and Vigezzi [20]. This was done in an effort to capture only the primary γ -transition. Further, contributions from the $(n, n'\gamma)$ channel can be neglected when considering γ rays in this energy range. The number of γ -cascades obtained using

the statistical γ -decay tagging technique is formally expressed as follows

$$N_{\beta\gamma}^{stat}(E_x) = \int_{6 \text{ MeV}}^{7 \text{ MeV}} \frac{N'_{\beta\gamma}(E_x, E_\gamma)}{\epsilon(E_\gamma)} dE_\gamma P_{stat}. \quad (6)$$

Here, P_{stat} represents the probability that the primary γ -transition lies within the energy range between 6–7 MeV and that this γ -ray energy gate does not also capture secondary and/or higher-order transitions.

If $P_{disc} = 1$, then $N_{\beta\gamma}^{disc}(E_x)$ is a perfect tag for the γ -decay channel (i.e., all cascades pass through the γ -transition of interest). If $P_{stat} = 1$, then $N_{\beta\gamma}^{stat}(E_x)$ is a perfect tag for the γ -decay channel (i.e., the 6–7 MeV γ -ray energy gate captures only the primary transition from every γ -cascade). The challenge in tagging the γ -decay channel lies in quantifying P_{disc} and P_{stat} . These terms can be investigated using empirical data or statistical models such as the DICEBOX code [21]. Alternatively, they can be fixed by normalization of the γ -decay probabilities using the assumption of unit probability below the neutron separation energy, because γ -ray emission is the only open decay channel. To investigate the ability of the discrete and statistical tagging methods to capture the γ -decay channel, the P_{disc} and P_{stat} terms in this work are assumed to be unity. For P_{disc} , this is unlikely as many low-lying transitions in ^{93}Mo and ^{95}Mo are in parallel. For P_{stat} , this assumption would require that all γ rays in the integration window of 6–7 MeV are primary transitions and that there are no primary transitions outside of this γ -ray energy range, also an unlikely assumption. However, these assumptions provide a foundation upon which to explore the areas of applicability of discrete and statistical tagging techniques for the surrogate neutron capture cross sections examined here.

In the external SRM, neutron-induced capture cross sections involving two different compound nuclei, denoted by the superscripts (1) and (2), are measured relative to one another:

$$\frac{\sigma_{(n,\gamma)}^{(1)}(E_n)}{\sigma_{(n,\gamma)}^{(2)}(E_n)} = \frac{\sigma_n^{(1)}(E_n) P_{\beta\gamma}^{(1)}(E_x^{(1)})}{\sigma_n^{(2)}(E_n) P_{\beta\gamma}^{(2)}(E_x^{(2)})}. \quad (7)$$

In previous applications of the external SRM, the neutron-induced compound nuclear formation cross sections, denoted $\sigma_n(E_n)$ in Eq. 7, were assumed to be equal for the two compound nuclei and thus, to cancel in the ratio. However, given the proximity to the $N = 50$ neutron shell closure, the neutron-induced compound formation cross sections for this work were obtained via optical model calculations. The uncertainty in both formation cross sections was approximated as 10% over the entire equivalent neutron energy range examined; however, this is likely an overestimate as a ratio analysis of two neighboring targets may involve correlated errors in the numerator and denominator.

Further, in previous applications of the external SRM, it was assumed that $\sigma_\beta(E_x)$ (See Eq. 4) is equal for two

surrogate reactions employed in the ratio as a function of excitation energy in the compound nuclei at and near the neutron separation energy and cancels in the ratio analysis. This is a reasonable assumption when target pairs are mid-shell deformed nuclei with similar nuclear structure (i.e., both even-even nuclei or both even-odd nuclei, with similar deformation and mass), but may fail in the consideration of dissimilar target pairs, particularly when target nuclei are at or near closed shells. Further, the (d, p) direct interaction has a Q-value dependence and this translates to a Q-value dependence on the direct reaction formation cross section. For this work, the $^{92}\text{Mo}(d, p)$ and $^{94}\text{Mo}(d, p)$ reactions have Q values of 5.845 MeV and 5.145 MeV, respectively, further suggesting a possible disparity in the direct reaction formation cross sections. Thus, in this application of the SRM, the total number of $^{92}\text{Mo}(d, p)$ and $^{94}\text{Mo}(d, p)$ reaction events was measured directly and explicitly taken into account in the determination of the $^{92}\text{Mo}(n, \gamma)$ surrogate ratio cross section.

III. EXPERIMENTAL DETAILS

An 11 MeV deuteron beam from the 88-Inch Cyclotron at Lawrence Berkeley National Laboratory was employed in the experiment. Data were taken over a period of 7 days with beam intensity fluctuating between 4 and 6 enA. The ^{92}Mo and ^{94}Mo targets were self-supporting metallic foils with areal densities of $460 \pm 5 \mu\text{g}/\text{cm}^2$ and $250 \pm 6 \mu\text{g}/\text{cm}^2$, respectively. The isotopic composition of the ^{92}Mo target is given in Table I. The ^{94}Mo target was approximately 95% isotopically pure.

The reaction products were detected using STARS/LiBerACE [22]. STARS was comprised of a 150 μm ΔE detector and a 1000 μm E detector, biased with 43 V and 170 V, respectively. The ^{92}Mo target was located 9 mm upstream from the front face of the ΔE detector with the particle telescope covering a forward angular range of approximately 52° to 75° relative to the beam axis. The ^{94}Mo target was located 21 mm upstream from the front face of the ΔE detector with the particle telescope covering a forward angular range of approximately 29° to 59° relative to the beam axis. The ΔE and E detectors were spaced approximately 2 mm apart. A 12.5- μm -thick aluminum shield was placed in front of the particle telescope to mitigate the effect of δ electrons. The configuration of the five Compton-suppressed HPGe detectors employed in this experiment is described in detail in Ref. [19].

The dissimilar target- ΔE spacing for the ^{92}Mo and ^{94}Mo targets is atypical for a surrogate ratio measurement and results in disparate sampling of ℓ -transfers for the two targets. To investigate this, distorted-wave Born approximation calculations were performed using DWUCK4 [23]. Calculations of the $^{92,94}\text{Mo}(d, p)$ cross section were obtained at an excitation energy corresponding to positive equivalent neutron energy with ℓ -transfers

TABLE I: Isotopic Composition of the ^{92}Mo Target

Isotope	Atomic Percent	Precision
92	98.27	± 0.10
94	0.46	± 0.05
95	0.37	± 0.03
96	0.26	± 0.03
97	0.13	± 0.03
98	0.27	± 0.03
100	0.25	± 0.03

of $\ell = 0$ up to the classical limit of $\ell = r \times p \approx 9$, averaged over the angle ranges relevant for the two target nuclei. The results suggest that the disparate angle ranges probed could result in angular momentum populations distributions that differ for the two residual nuclei by as much as a factor of three. If the Weisskopf-Ewing approximation is not applicable, the disparate angular momentum population distributions for the two residual nuclei employed in the ratio measurement may introduce uncorrelated error in the surrogate ratio measurement.

IV. RESULTS AND DISCUSSION

A two-dimensional, proton-gated matrix of γ -ray energy and compound nuclear excitation energy, E_x , was obtained for both the $^{92}\text{Mo}(d,p)$ and $^{94}\text{Mo}(d,p)$ reactions. Non-statistical uncertainty in the compound nuclear excitation energy data is dominated by the intrinsic detector resolution (See Ref. [6] for more detail) and was estimated as approximately 200 keV (FWHM). For each excitation energy bin in the compound nucleus, γ -ray spectra covering an energy range of approximately 100 keV to 8 MeV were recorded and each γ -ray spectrum was convolved with the absolute γ -ray detection efficiency of the HPGe array.

To investigate possible target contamination in the determination of the total number of surrogate reaction events, $N_\beta(E)$, the discrete γ -decay spectra for the ^{93}Mo and ^{95}Mo compound nuclei were examined for pollution from carbon and oxygen contaminants. The presence of γ rays from the $^{12}\text{C}(d,p)^{13}\text{C}$ reaction at energies below 4 MeV prompted further investigation via generation of a Doppler-shifted γ -ray spectrum adapted to reactions on carbon. To explore the contribution of $^{12}\text{C}(d,p)^{13}\text{C}$ events to $N_\beta(E)$, the number of protons in coincidence with both the 3684.5 keV and 3853.8 keV ^{13}C γ rays were determined for the $^{92,94}\text{Mo}(d,p)$ data sets, corrected for γ -ray detection efficiency, branching ratio and Mo data “background” contributions and then compared to the total number of particle singles events in the same energy range. Contribution from carbon contamination was determined to comprise no more than $\approx 1\%$ of the total singles spectrum in the excitation energy range relevant for the surrogate cross section measurement. Given that there are no conflicting ^{13}C γ rays observed in the γ -ray energy regions of interest, no carbon contamination was

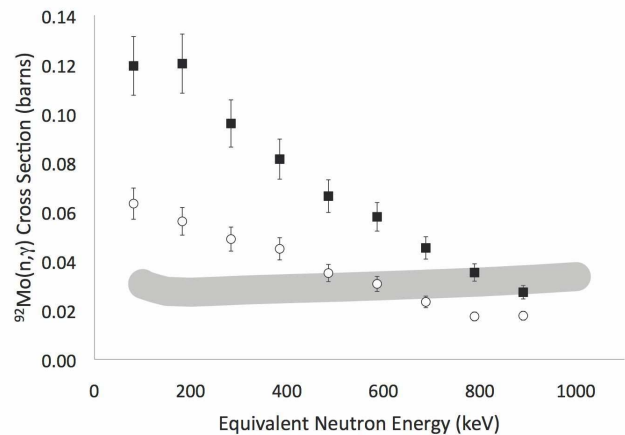


FIG. 1: The $^{92}\text{Mo}(n,\gamma)$ cross section extracted via the absolute surrogate technique using the discrete (open circles) and statistical (filled squares) γ -decay techniques as a function of equivalent neutron energy obtained via the (d,p) surrogate reaction. The error bars represent both the statistical and nonstatistical uncertainty. For comparison, the evaluated $^{92}\text{Mo}(n,\gamma)$ cross section from ENDF/B-VII.0 with associated uncertainty is denoted by the shaded region.

present in the particle- γ coincident data relevant for the surrogate cross section measurements.

A. Absolute surrogate measurement

Figure 1 shows the $^{92}\text{Mo}(n,\gamma)$ cross section obtained via the absolute surrogate method as described in Eq. 1 as a function of equivalent neutron energy. Both the discrete (open circles) and statistical (filled squares) γ -decay tagging techniques were employed. The shaded region represents the evaluated $^{92}\text{Mo}(n,\gamma)$ cross section obtained from ENDF/B-VII.0 [24] with associated 18% uncertainty [25]. The uncertainty in the ^{92}Mo neutron-induced compound formation cross section contributes approximately 10% to the non-statistical uncertainty in the surrogate measurements. The absolute surrogate cross sections obtained using both the discrete and statistical γ -decay tagging technique deviate from the ENDF/B-VII.0 evaluation (despite the isolated agreement for the discrete $^{92}\text{Mo}(n,\gamma)$ surrogate cross section between 480 and 690 keV and for the statistical $^{92}\text{Mo}(n,\gamma)$ surrogate cross section between 790 and 890 keV) and exhibit an inconsistent shape. These discrepancies between the surrogate and evaluated data may imply a failure of the Weisskopf-Ewing approximation required to obtain Eq. 1 and/or that the P_{stat} and P_{disc} terms in Eqs. 5 and 6, respectively, deviate from unity and vary with excitation energy. This is further explored in Sec. IV C.

To constrain P_{stat} , simulation to quantify the appropriate γ -ray energy range to isolate primary γ -transitions is needed. Similarly, P_{disc} can be constrained with an evaluation of parallel γ -decay paths. Further, the expres-

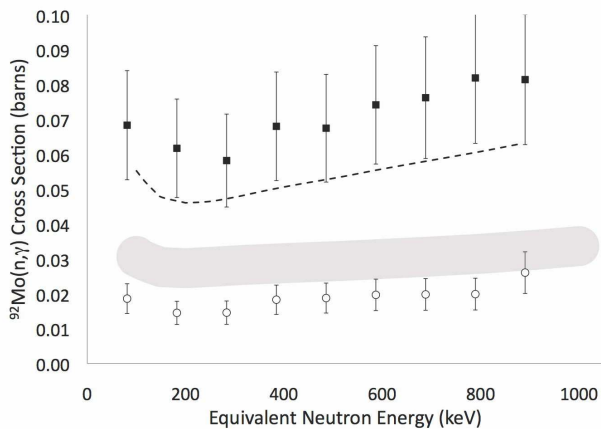


FIG. 2: The $^{92}\text{Mo}(n,\gamma)$ cross section extracted using the SRM relative to the evaluated $^{94}\text{Mo}(n,\gamma)$ cross section obtained from ENDF/B-VII.0 using the discrete (open circles) and statistical (filled squares) γ -decay techniques as a function of equivalent neutron energy obtained via the (d,p) surrogate reaction. The error bars represent both the statistical and nonstatistical uncertainty. For comparison, the evaluated $^{92}\text{Mo}(n,\gamma)$ cross section from ENDF/B-VII.0 with associated uncertainty is denoted by the shaded region. The evaluated $^{94}\text{Mo}(n,\gamma)$ cross section from ENDF/B-VII.0 is denoted by the dashed line.

sions in Eqs. 1 and 2 are based on the assumption that a compound system has been formed. However, there is a finite probability that the neutron leaks out of the system before the compound nucleus is formed. A study of radiative capture indicates that these effects can be quite large, approximately 10 – 15% overall and up to 50% for low partial waves [26]. Neutron leakage into the continuum may result in an ostensibly larger number of direct reaction events that actually go on to form the compound nucleus.

B. Surrogate ratio measurement

To determine the ratio of the surrogate γ -decay probabilities, as outlined in Eq. 7, the ratio of the number of proton- γ coincident events was obtained. The ratio data were multiplied by the ENDF/B-VII.0 $^{94}\text{Mo}(n,\gamma)$ cross sections as described in Eq. 7 to obtain the $^{92}\text{Mo}(n,\gamma)$ cross section. The surrogate $^{92}\text{Mo}(n,\gamma)$ cross section obtained using the ENDF/B-VII.0 $^{94}\text{Mo}(n,\gamma)$ reference cross section evaluation is shown in Fig. 2, with the open circles and filled squares representing surrogate data obtained using the discrete and statistical γ -decay tagging techniques, respectively. For reference, the dashed line represents the evaluated $^{94}\text{Mo}(n,\gamma)$ cross section obtained from ENDF/B-VII.0. The shaded region again represents the evaluated $^{92}\text{Mo}(n,\gamma)$ cross section obtained from ENDF/B-VII.0 with associated 18% uncertainty. Note that no experimental data exist above 125 keV to support the $^{92}\text{Mo}(n,\gamma)$ cross section evaluation (i.e.,

the evaluation above 125 keV is based on calculation alone). The sources of non-statistical uncertainty in the $^{92}\text{Mo}(n,\gamma)$ cross section surrogate ratio data include the uncertainty in the neutron-induced compound formation cross sections ($\approx 10\%$) and uncertainty in the $^{94}\text{Mo}(n,\gamma)$ reference cross section evaluation ($\approx 20\%$). It is important to note that the error due to the neutron-induced compound formation cross section calculations is likely a conservative estimate, given that the ratio involved two neighboring targets with possible correlated errors in the numerator and the denominator. The largest source of non-statistical uncertainty in previous applications of the SRM utilizing the statistical γ -ray tagging technique – contributions from possible isotopic contamination – is removed given the ability to analyze target composition using discrete γ -transitions.

The surrogate ratio $^{92}\text{Mo}(n,\gamma)$ cross section obtained using the discrete γ -decay technique exhibits a similar shape as the ENDF/B-VII.0 evaluation, but is systematically lower by a factor of 1.5 to 2 for the range of equivalent neutron energies probed (excluding the isolated agreement of the data point at 890 keV). Here, the two transitions used in the discrete tag, for ^{93}Mo at 943.28 keV ($1/2^+ \rightarrow 5/2^+$) and for ^{95}Mo at 204.12 keV ($3/2^+ \rightarrow 5/2^+$), have different initial spins. This may introduce error in the measurement if the Weisskopf-Ewing approximation is not applicable. Ideally, for the SRM, transitions with “equivalent” structure and energy should be utilized in a discrete tag. The surrogate $^{92}\text{Mo}(n,\gamma)$ cross section obtained using the statistical γ -decay technique is systematically higher than the ENDF/B-VII.0 evaluation by a factor of two to three for the range of equivalent neutron energies probed. The surrogate $^{92}\text{Mo}(n,\gamma)$ cross section obtained using the statistical γ -decay technique trends well with the $^{94}\text{Mo}(n,\gamma)$ fiducial cross section, indicating somewhat poor scaling of the reference cross section towards the “true” cross section.

It is important to note that the particle energy resolution (and thus compound nuclear excitation energy resolution) is approximately 200 keV and thus, the surrogate data at 80 keV may contain contributions from negative equivalent neutron energy. The decreased low-energy level density for the quasi-spherical compound nuclei examined here makes failure of the Weisskopf-Ewing approximation likely and agreement of the surrogate data with the evaluated data at low equivalent neutron energies is unexpected if the surrogate ratio measurement is inaccurate due to breakdown of the Weisskopf-Ewing approximation. In that case, the greatest deviations from the evaluated data would be *expected* to occur at lower equivalent neutron energy and the surrogate data would be more likely to converge with the evaluated data as equivalent neutron energy increases. Despite the disparities, the reasonable agreement of the $^{92}\text{Mo}(n,\gamma)$ cross section obtained via the SRM and the evaluated data may indicate that possible correlated errors (e.g., effects of the angular momentum population distribution, neutron leakage into the continuum, etc.) cancel in the ratio

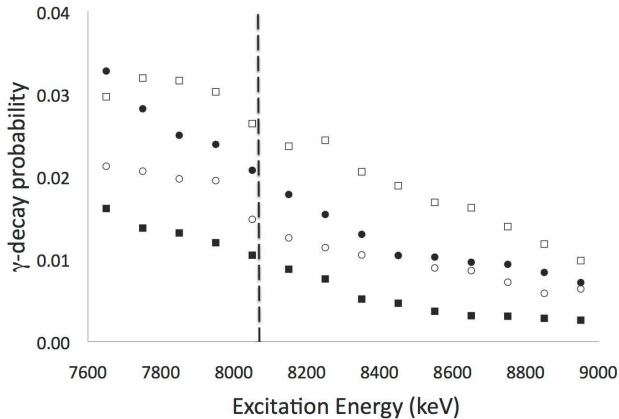


FIG. 3: The γ -decay probability of the ^{93}Mo (open symbols) and ^{95}Mo (filled symbols) residual nuclei obtained using the discrete (circles) and statistical (squares) γ -decay techniques as a function of excitation energy in the residual nucleus. The dashed line represents the neutron separation energy of the ^{93}Mo compound nucleus ($S_n = 8.06981$ MeV). The statistical error is smaller than the data points.

analysis.

C. Comparison of γ -decay tagging techniques

Further investigation of the discrete and statistical γ -decay tagging techniques led to exploration of the γ -decay probabilities of the ^{93}Mo and ^{95}Mo residual nuclei. As shown in Fig. 3 and outlined in Eq. 2, the γ -decay probability of the ^{93}Mo (open symbols) and ^{95}Mo (filled symbols) residual nuclei was obtained using the discrete and statistical γ -decay techniques as a function of excitation energy in the residual nuclei. The γ -decay probabilities obtained for ^{95}Mo are larger using the discrete γ -decay tagging technique as compared to the statistical γ -decay tagging technique. However, the γ -decay probabilities obtained for ^{93}Mo exhibit the opposite trend. This indicates that the two methods for tagging the γ -decay channel capture different information (i.e., that the P_{stat} and P_{disc} terms in Eqs. 5 and 6, respectively, differ significantly for these quasi-spherical residual nucleus).

The dashed line in Fig. 3 represents the neutron separation energy in the ^{93}Mo residual nucleus ($S_n = 8.06981$ MeV). As the excitation energy in the ^{93}Mo residual nucleus increases beyond the neutron separation energy, the γ -decay probability is expected to decrease with the opening of the neutron emission channel. This is evidenced by the smooth decrease in the γ -decay probabilities obtained using the both the discrete and statistical γ -decay tagging techniques beyond the neutron separation energy. Below the neutron separation energy, the only open decay channel is γ -decay and thus, the assumption of $P_{disc} = P_{stat} = 1$ implies that the γ -decay probabilities below the neutron separation energy are ex-

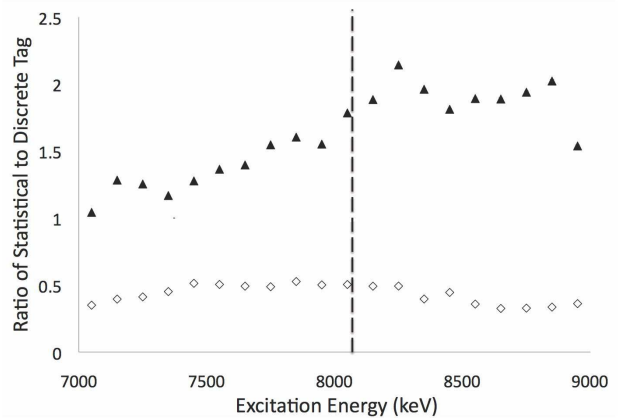


FIG. 4: Ratio of the statistical to discrete γ -decay tags as a function of excitation energy in the ^{93}Mo (filled triangles) and ^{95}Mo (open diamonds) residual nuclei. The dashed line represents the neutron separation energy in the ^{93}Mo compound nucleus. In some cases, the statistical error is smaller than the data points.

pected to be unity. For both the discrete and statistical tagging techniques, however, the measured γ -decay probabilities for the ^{93}Mo residual nucleus are much less than unity below the neutron separation energy, indicating incomplete collection of the γ -decay channel for both tagging techniques.

Figure 4 shows the ratio of the number of γ rays emitted in the 6–7 MeV energy range to the number of counts in the γ -ray transition of interest for the ^{93}Mo (filled triangles) and ^{95}Mo (open diamonds) residual nuclei. A constant value for this ratio as a function of excitation energy would suggest that the same information is contained in the discrete and statistical γ -ray tags. If either tagging method is significantly influenced by the initial angular momentum population distribution, it is unlikely that a constant value will be obtained for this ratio as a function of excitation energy.

Over an excitation energy range of 7.6 MeV to 9 MeV, this ratio for the ^{93}Mo residual nucleus varies from a minimum value of 1.396 ± 0.003 to a maximum value of 2.142 ± 0.008 . Over the same excitation energy range, this ratio for the ^{95}Mo residual nucleus remains roughly constant between a minimum of 0.325 ± 0.001 and a maximum of 0.526 ± 0.003 . The increased variability of this ratio for the ^{93}Mo residual nucleus is reasonable. In the limit of the weak coupling model [27], the nuclear levels in ^{93}Mo can be described by the coupling of the odd neutron to the ^{92}Mo even-even core ($Z = 42$, $N = 50$). The first excited state in ^{92}Mo lies at an excitation energy of 1509.5 keV. In ^{93}Mo , γ -ray transitions below this excitation energy likely involve discrete nuclear structure. The state used to tag the γ -decay channel in ^{93}Mo is at 943.28 keV and the discrete γ -ray tagging method may be more sensitive to the angular momentum population distribution for nuclei near closed shells.

V. CONCLUSIONS

We have indirectly measured the $^{92}\text{Mo}(n,\gamma)$ cross section over an equivalent neutron energy range of 80 keV to 890 keV, showcasing the first use of the surrogate method in the determination of neutron capture cross section data on spherical and near-spherical nuclei in the mass-90 region. The data exhibit a failure of the absolute surrogate technique and indicate that the SRM tends to minimize correlated errors in the measurement, regardless of the employed γ -decay tagging technique. To obtain an accurate surrogate measurement of the $^{92}\text{Mo}(n,\gamma)$ cross section using the discrete tagging technique, empirical data could be used to sum parallel γ -decay paths (cf. Ref. [9]). For the statistical tagging technique, a model-dependent approach may be necessary to estimate angular momentum population distributions and constrain the γ -ray energy range to isolate primary γ -transitions. A comparison of the discrete and statistical tagging methods indicate that these techniques are more likely to capture similar information for more deformed nuclei. Future work should include a comprehensive theoretical treatment of the surrogate method, specifically in the evaluation of the discrete and statistical γ -ray tagging techniques.

Acknowledgments

We thank the 88-Inch Cyclotron operations and facilities staff for their help in performing these experiments. This work was supported, in part, by the University of California, Berkeley Chancellor's Postdoctoral Fellowship Program and the Clare Boothe Luce Foundation and performed under the auspices of the Berkeley Nuclear Research Center (BNRC) through the 00F8F4 University of California Lab Fees Research Program. This work was also performed under the auspices of the U.S. Department of Energy by the University of Richmond under Grant Nos. DE-FG52-06NA26206 and DE-FG02-05ER41379, Lawrence Livermore National Laboratory under Contract No. DE-AC52-07NA27344 and Lawrence Berkeley National Laboratory under Contract No. DE-AC02-05CH11231. MW acknowledges support from the National Research Foundation of South Africa.

-
- [1] C. Plettner, H. Ai, C.W. Beausang, L.A. Bernstein, L. Ahle, H. Amro, M. Babilon, J.T. Burke, J.A. Caggiano, R.F. Casten, *et al.*, Phys. Rev. C **71**, 051602(R) (2005).
- [2] J.T. Burke, L.A. Bernstein, J. Escher, L. Ahle, J.A. Church, F.S. Dietrich, K.J. Moody, E.B. Norman, L. Phair, P. Fallon, *et al.*, Phys. Rev. C **73**, 054604 (2006).
- [3] B.F. Lyles, L.A. Bernstein, J.T. Burke, F.S. Dietrich, J. Escher, I. Thompson, D.L. Bleuel, R.M. Clark, P. Fallon, J. Gibelin, *et al.*, Phys. Rev. C **76**, 014606 (2007).
- [4] M.S. Basunia, R.M. Clark, B.L. Goldblum, L.A. Bernstein, L. Phair, J.T. Burke, C.W. Beausang, D.L. Bleuel, B. Darakchieva, F.S. Dietrich, M. Evtimova, P. Fallon, J. Gibelin, R. Hatarik, C.C. Jewett, S.R. Leshner, M.A. McMahan, E. Rodriguez-Vieitez, M. Wiedeking, Nucl. Instrum. Meth. B **267**, 1899 (2009).
- [5] S. R. Leshner, J. T. Burke, L. A. Bernstein, H. Ai, C. W. Beausang, D. L. Bleuel, R. M. Clark, F. S. Dietrich, J. E. Escher, P. Fallon, J. Gibelin, B. L. Goldblum, I. Y. Lee, A. O. Macchiavelli, M. A. McMahan, K. J. Moody, E. B. Norman, L. Phair, E. Rodriguez-Vieitez, N. D. Scielzo, and M. Wiedeking, Phys. Rev. C **79**, 044609 (2009).
- [6] B. L. Goldblum, S. R. Stroberg, J. M. Allmond, C. Angell, L. A. Bernstein, D. L. Bleuel, J. T. Burke, J. Gibelin, L. Phair, N. D. Scielzo, E. Swanberg, M. Wiedeking, and E. B. Norman, Phys. Rev. C **80**, 044610 (2009).
- [7] J.J. Ressler, J.T. Burke, J.E. Escher, C.T. Angell, M.S. Basunia, C.W. Beausang, L.A. Bernstein, D.L. Bleuel, R.J. Casperson, B.L. Goldblum, J. Gostic, R. Hatarik, R. Henderson, R.O. Hughes, J. Munson, L.W. Phair, T.J. Ross, N.D. Scielzo, E. Swanberg, I.J. Thompson and M. Wiedeking, Phys. Rev. C **83**, 054610 (2011).
- [8] S. Boyer, D. Dassié, J.N. Wilson, M. Aiche, G. Barreau, S. Czajkowski, C. Grosjean, A. Guiral, B. Haas, B. Osmanov, G. Aerts, E. Berthoumieux, F. Gunsing, Ch. Theisen, N. Thiollière and L. Perrot, Nucl. Phys. A **775**, 175 (2006).
- [9] J.M. Allmond, L.A. Bernstein, C.W. Beausang, L. Phair, D.L. Bleuel, J.T. Burke, J.E. Escher, K.E. Evans, B.L. Goldblum, R. Hatarik, H.B. Jeppesen, S.R. Leshner, M.A. McMahan, J.O. Rasmussen, N.D. Scielzo and M. Wiedeking, Phys. Rev. C **79**, 054610 (2009).
- [10] R. Hatarik, L.A. Bernstein, J.A. Cizewski, D.L. Bleuel, J.T. Burke, J.E. Escher, J. Gibelin, B.L. Goldblum, A.M. Hatarik, S.R. Leshner, P.D. O'Malley, L. Phair, E. Rodriguez-Vieitez, T. Swan and M. Wiedeking, Phys. Rev. C **81**, 011602(R) (2010).
- [11] N.D. Scielzo, J.E. Escher, J.M. Allmond, M.S. Basunia, C.W. Beausang, L.A. Bernstein, D.L. Bleuel, J.T. Burke, R.M. Clark, F.S. Dietrich, P. Fallon, J. Gibelin, B.L. Goldblum, S.R. Leshner, M.A. McMahan, E.B. Norman, L. Phair, E. Rodriguez-Vieitez, S.A. Sheets, I.J. Thompson, and M. Wiedeking, Phys. Rev. C **81**, 034608 (2010).
- [12] B.L. Goldblum, S.G. Prussin, U. Agvaanluvsan, L.A. Bernstein, D.L. Bleuel, W. Younes and M. Guttormsen, Phys. Rev. C **78**, 064606 (2008).
- [13] B.L. Goldblum, S.G. Prussin, L.A. Bernstein, W. Younes, M. Guttormsen and H.T. Nyhus, Phys. Rev. C **81**, 054606 (2010).
- [14] P. Paradis, G. Lamoureux, R. Lecomte and S. Monaro, Phys. Rev. C **14**, 835 (1976).
- [15] V.F. Weisskopf and D.H. Ewing, Phys. Rev. **57**, 472 (1940).
- [16] J.E. Escher and F.S. Dietrich, Phys. Rev. C **81**, 024612 (2010).
- [17] H.C. Britt and J.B. Wilhelmy, Nucl. Sci. Engr. **72**, 222 (1979).
- [18] A.J. Koning and J.-P. Delaroche, Nucl. Phys. A **713**, 231 (2003).
- [19] M. Wiedeking, L.A. Bernstein, M. Krčička, D.L. Bleuel, J.M. Allmond, M.S. Basunia, J.T. Burke, P. Fallon, R.B. Firestone, B.L. Goldblum, R. Hatarik, P.T. Lake, I-Y. Lee, S.R. Leshner, S. Paschalis, M. Petri, L. Phair and N.D. Scielzo, Phys. Rev. Lett. **108**, 162503 (2012).
- [20] T. Døssing, E. Vigezzi Nucl. Phys. A **587** (1995) 13-35.
- [21] F. Bečvář, Nucl. Instrum. Methods A **417**, 434 (1998).
- [22] S.R. Leshner, L. Phair, L.A. Bernstein, D.L. Bleuel, J.T. Burke, J.A. Church, P. Fallon, J. Gibelin, N.D. Scielzo and M. Wiedeking, Nucl. Instrum. Meth. A **621**, 286 (2010).
- [23] P.D. Kunz, DWUCK4 - A Zero Range Distorted Wave Born Approximation Program, University of Colorado (unpublished).
- [24] M.B. Chadwick, P. Oblozinsky, M. Herman, N.M. Greene, R.D. McKnight, D.L. Smith, P.G. Young, R.E. MacFarlane, G.M. Hale, S.C. Frankle, *et al.*, "ENDF/B-VII.0: Next Generation Evaluated Nuclear Data Library for Nuclear Science and Technology," *Nuclear Data Sheets*, **107**, 2931-3060, 2006.
- [25] S.F. Mughabghab (private communication).
- [26] F.S. Dietrich, in *Proceedings of the International Workshop on Compound-Nuclear Reactions and Related Topics, Yosemite, California, 2007*, (AIP Conf. Proc. 1005, 2008), p. 125.
- [27] A. Arima and I. Hamamoto, Ann. Rev. Nucl. Sci. **21**, 55 (1971).